## SUPPLEMENTAL MATERIAL

**Diamond et al., http://www.jem.org/cgi/content/full/jem.20101158/DC1**

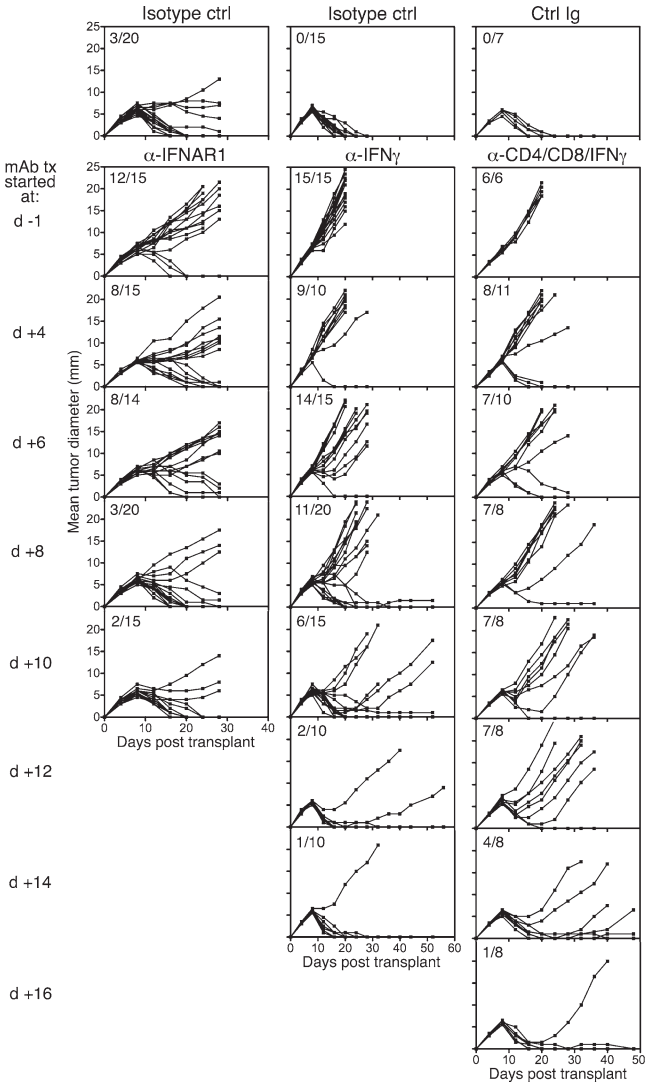


**Figure S1. Kinetics of H31m1 tumor growth after antibody-mediated IFN-α/β receptor blockade at different times.** WT mice injected with $10^6$ H31m1 tumor cells (at day 0) were treated with anti-IFNAR1, anti–IFN-γ, or anti-CD4/CD8/IFN-γ mAbs beginning on the indicated day, and tumor growth was monitored over time. Each line represents growth in an individual mouse, with the fraction of tumor-positive mice per group (defined as >6 × 6 mm in diameter at the end of observation) indicated. Similar numbers of mice were treated in parallel with the corresponding isotype control mAb at all time points, although only one representative graph for each control is shown. The data represent cumulative results from two to four independent experiments with group sizes as indicated. Antibody treatment regimens were used as described in Materials and methods.

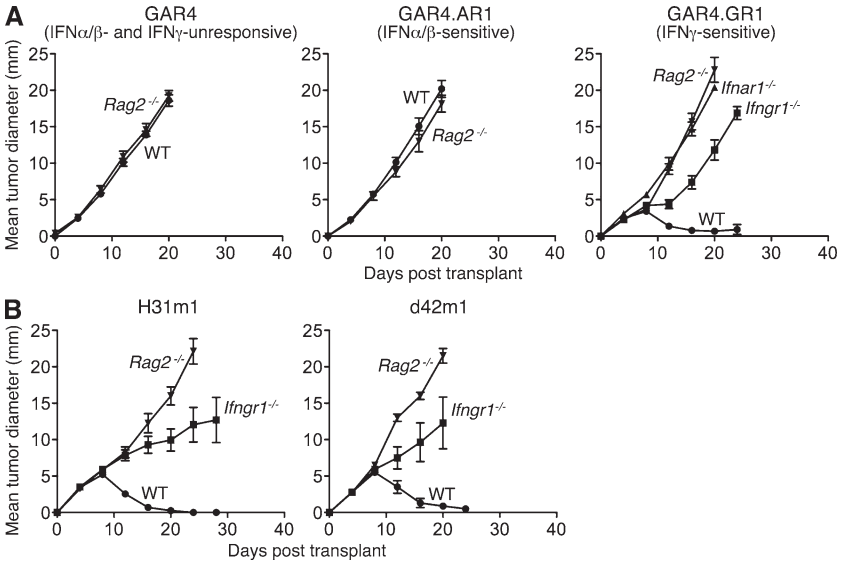


**Figure S2. IFN-γ responsiveness in host cells as well as the tumor is required for rejection of highly immunogenic sarcomas.** (A) WT, *Rag2*$^{-/-}$, *Ifngr1*$^{-/-}$, and *Ifnar1*$^{-/-}$ mice were injected s.c. with $10^6$ GAR4 (MCA sarcoma derived from *Ifngr1*$^{-/-}$*Ifnar1*$^{-/-}$ mice, unresponsive to IFN-α/β and IFN-γ), IFN-α/β–sensitive GAR4.AR1 (IFNAR1 transduced), or IFN-γ–sensitive GAR4.GR1 (IFNGR1 transduced) tumor cells, and growth was monitored over time. Data represent mean tumor diameter ± SEM from at least two independent experiments with 5–11 mice/group. (B) WT, *Rag2*$^{-/-}$, and *Ifngr1*$^{-/-}$ mice were injected s.c. with $10^6$ H31m1 or d42m1 unedited MCA sarcoma cells, and growth was measured over time. Mean tumor diameter ± SEM is shown for groups of 5–12 WT or *Ifngr1*$^{-/-}$ mice and 2–4 *Rag2*$^{-/-}$ mice.

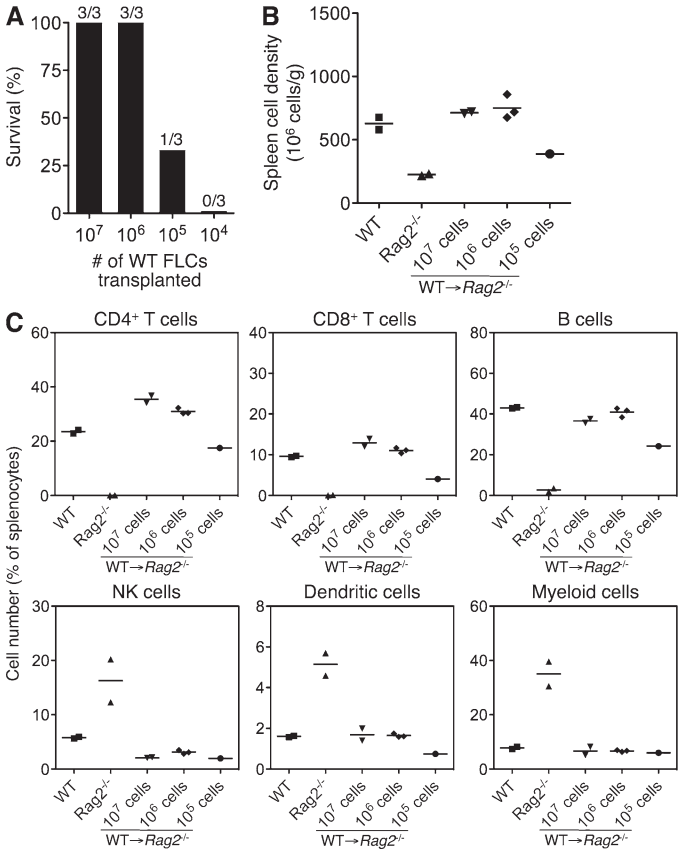


**Figure S3. Titration of unfractionated FLCs for hematopoietic reconstitution of lethally irradiated recipients.** (A–C) WT FLCs at the indicated dose were transplanted by i.v. injection into irradiated *Rag2*$^{-/-}$ recipients, and mice were monitored for survival (A) and hematopoietic reconstitution at 12 wk after transplantation (B and C). Spleens from WT and *Rag2*$^{-/-}$ control mice and surviving WT → *Rag2*$^{-/-}$ chimeras were harvested and assessed for cell density (total cell number/wt of tissue; B) as well as percentages of immune cell subsets (C). Cell populations were defined as follows: CD4$^+$ T cells (CD3$^+$CD4$^+$), CD8$^+$ T cells (CD3$^+$CD8$^+$), B cells (B220$^+$), NK cells (DX5$^+$CD3$^-$), DCs (CD11c$^{hi}$), and myeloid cells (CD11b$^+$). For subsequent experiments, a dose of $5 \times 10^6$ FLCs was used to generate bone marrow chimeras. Data are representative of at least two independent experiments. (B and C) Horizontal bars represent the mean.

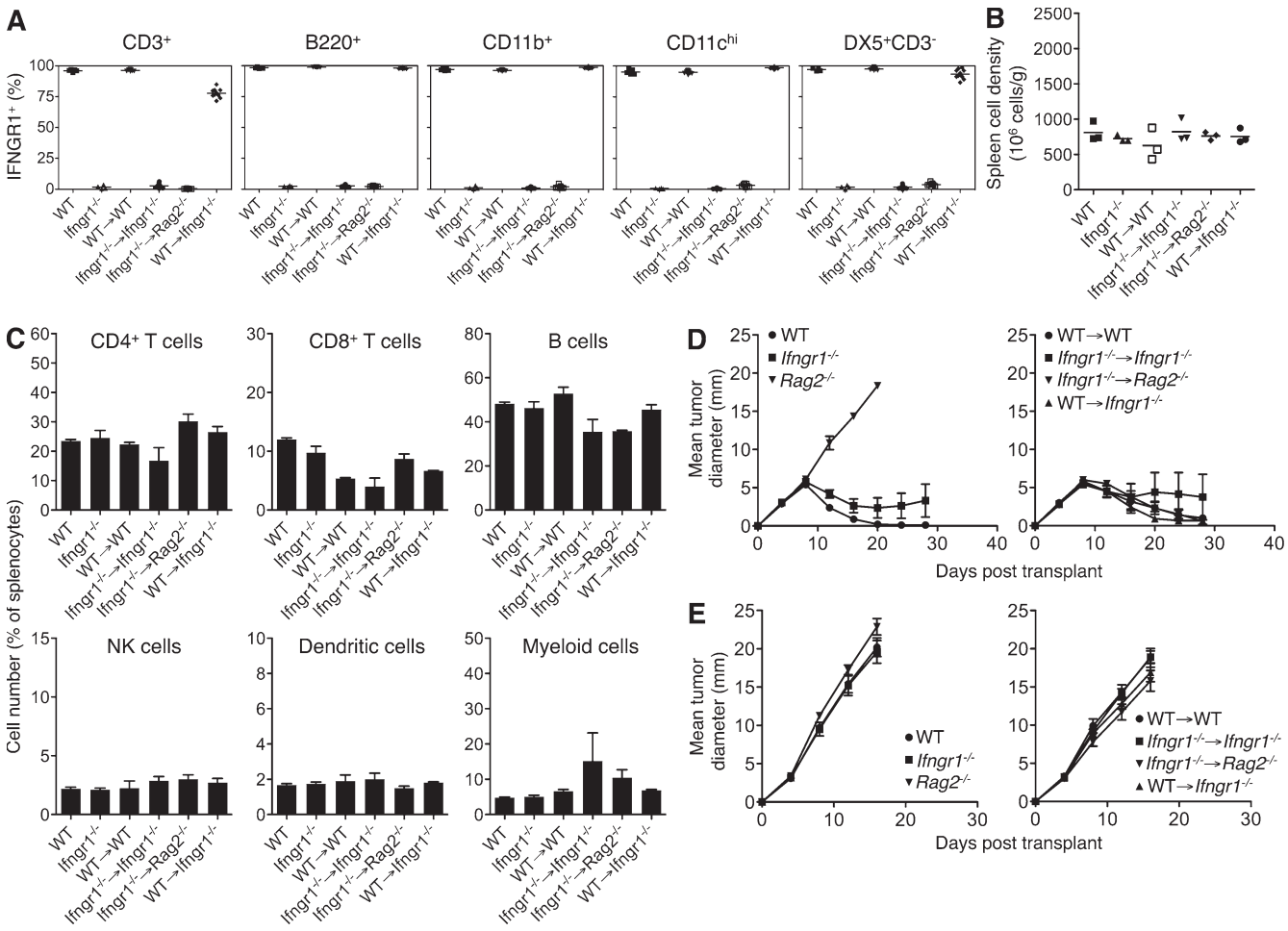


**Figure S4. Normal functional immune reconstitution in *Ifngr1*$^{-/-}$ bone marrow chimeric mice.** (A) Splenocytes from representative cohorts of control and chimeric mice were harvested and analyzed for IFNGR1 expression by flow cytometry. The percentage of IFNGR1$^+$ cells among splenocytes in the indicated gate (CD3$^+$, B220$^+$, CD11b$^+$, CD11c$^{hi}$, or DX5$^+$CD3$^-$) is plotted for 4–5 control mice and 7–12 chimeras of each type. (B) Cell density of the spleen is shown for three control and chimeric mice of each type. (A and B) Horizontal bars represent the mean. (C) Cellular percentages of the indicated immune cell subsets were determined by flow cytometry for control and chimeric mice. Mean values (as a percentage of total splenocytes) ± SEM for three mice/group are shown, and cell populations were defined as follows: CD4$^+$ T cells (CD3$^+$CD4$^+$), CD8$^+$ T cells (CD3$^+$CD8$^+$), B cells (B220$^+$), NK cells (DX5$^+$CD3$^-$), DCs (CD11c$^{hi}$), and myeloid cells (CD11b$^+$). (D) Control and chimeric mice were injected with $10^6$ F535 unedited MCA sarcoma cells, and growth was monitored over time. Mean tumor diameter ± SEM is plotted for 5–11 mice/group from two independent experiments. Error bars represent growth in 2/11 *Ifngr1*$^{-/-}$ mice and 1/6 *Ifngr1*$^{-/-}$ → *Ifngr1*$^{-/-}$ chimeras. (E) WT-derived 1877 tumor cells were injected at a dose of $10^6$ cells/mouse into groups of control and chimeric mice. Data represent mean tumor diameter ± SEM for four to five mice/group.

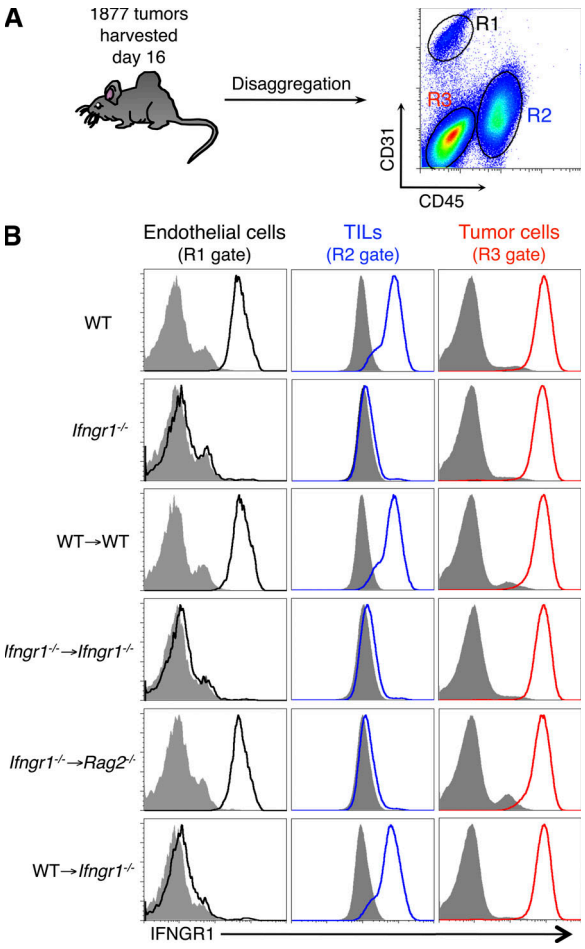


**Figure S5. Tumor-infiltrating leukocytes in *Ifngr1*$^{-/-}$ bone marrow chimeras are donor bone marrow derived, whereas tumor-associated endothelium is derived from nonhematopoietic host cells.** Tumors from control and chimeric mice were harvested 16 d after injection of $10^6$ 1877 sarcoma cells. After disaggregation, cell suspensions were stained with antibodies specific for CD45, CD31, and IFNGR1, and analyzed by flow cytometry. (A) A representative FACS plot shows CD45 and CD31 staining of a disaggregated tumor cell suspension, with endothelial cell ($CD31^+CD45^-$, R1), tumor-infiltrating leukocyte ($CD45^+CD31^-$, R2), and tumor cell ($CD45^-CD31^-$, R3) gates indicated. (B) IFNGR1 expression levels were assessed on individual cellular subsets from harvested tumors. Representative samples from control and bone marrow chimeric mice of each type are shown, with staining of irrelevant isotype control antibody in the shaded histograms. IFNGR1 staining on cells of the tumor served as an internal positive control. Additional experiments analyzing IFNGR1 levels on $CD3^+$, $CD11b^+$, and $CD11c^{hi}$ subsets within the tumor-infiltrating leukocytes (TILs) yielded results similar to those in the corresponding population isolated from the spleen (not depicted). Data are representative of at least two independent experiments.

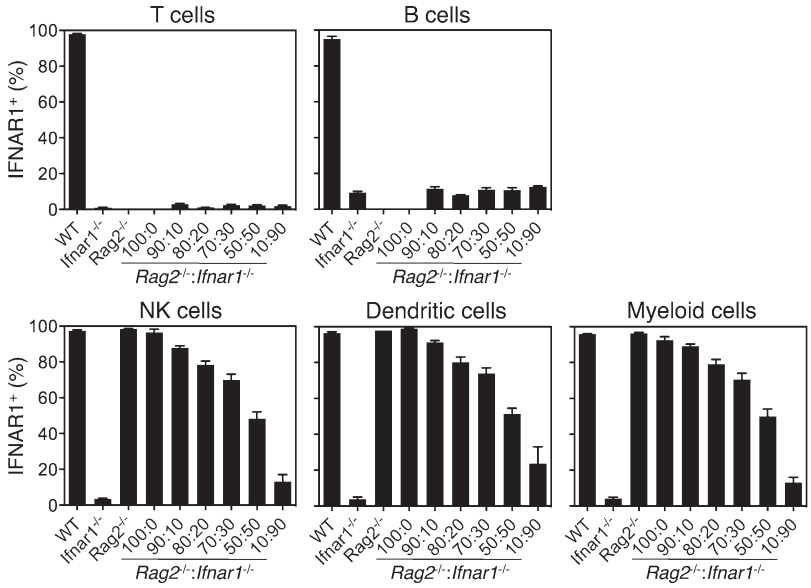


**Figure S6. Mixing ratio of *Rag2*$^{-/-}$ to *Ifnar1*$^{-/-}$ HSCs determines the fraction of IFN-α/β–responsive cells within the innate immune compartment of reconstituted mice.** Lethally irradiated *Rag2*$^{-/-}$ mice were injected i.v. with mixtures of *Rag2*$^{-/-}$ and *Ifnar1*$^{-/-}$ HSCs at the indicted ratios. At 10–12 wk after reconstitution, splenocytes were analyzed for expression of IFNAR1 within the following immune cell compartments: T cells (CD3$^{+}$), B cells (B220$^{+}$), NK cells (DX5$^{+}$CD3$^{-}$), DCs (CD11c$^{hi}$), and myeloid cells (CD11b$^{+}$). Similar results were obtained using either FLCs or 5-FU–treated adult bone marrow as a source of donor HSCs, and the data were pooled, representing two to eight mice at each ratio. Reconstitution of normal T cell percentages in the spleen was less consistently observed with the 90:10 ratio compared with the remaining ratios (not depicted); therefore, 80:20 mixtures were used for subsequent experiments. Error bars represent SEM.

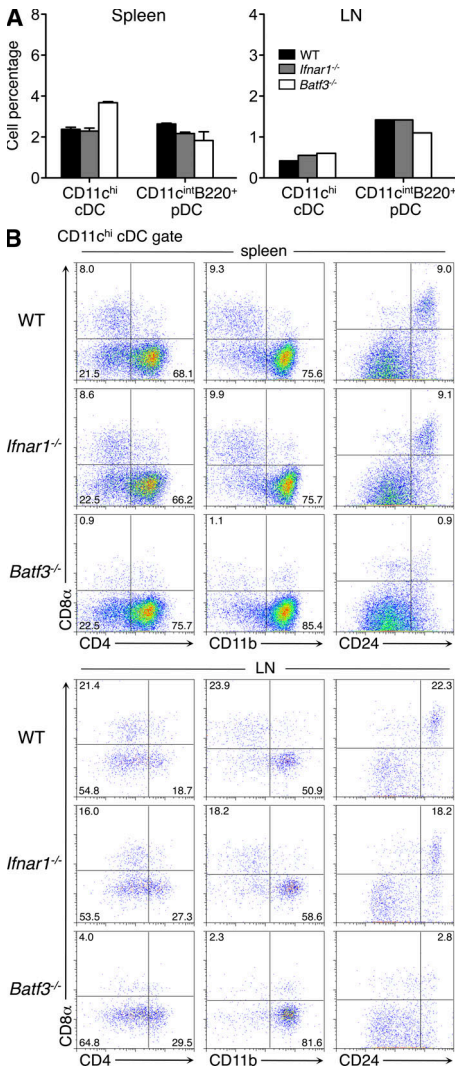


**Figure S7. Normal percentages of DC subsets in *Ifnar1*$^{-/-}$ mice.** Cells were isolated from the spleens and LNs of WT, *Ifnar1*$^{-/-}$, and *Batf3*$^{-/-}$ mice by collagenase digestion, and DC subsets were analyzed by flow cytometry. (A) Relative numbers (as a percentage of live cells) of CD11c$^{hi}$ conventional DCs (cDC) and CD11c$^{int}$B220$^{+}$ pDCs are shown. Data represent the mean ± SEM from four WT, four *Ifnar1*$^{-/-}$, and two *Batf3*$^{-/-}$ spleens or values from pooled inguinal LNs. (B) Splenocytes and LN cells were gated on CD11c$^{hi}$ conventional DCs and analyzed for CD8α, CD4, CD11b, and CD24 expression. FACS plots from a representative sample of WT, *Ifnar1*$^{-/-}$, and *Batf3*$^{-/-}$ splenocytes or pooled LN cells are shown. The percentage of cells in the indicated gates is noted.

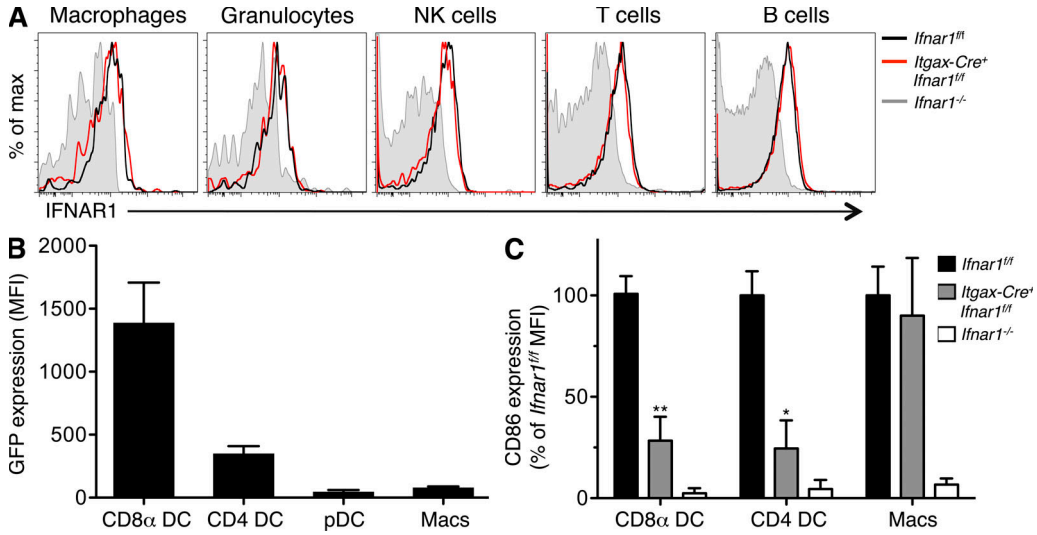


**Figure S8. Characterization of *Itgax-Cre*$^{+}$*Ifnar1*$^{f/f}$ mice.** (A) Comparable levels of IFNAR1 expression in non-DC subsets from of *Itgax-Cre*$^{+}$*Ifnar1*$^{f/f}$ and *Ifnar1*$^{f/f}$ mice by flow cytometry. Shown is a representative experiment from at least two independent experiments. (B) Increased expression of Cre recombinase in CD8α$^{+}$ DC. *Itgax-Cre*$^{+/-}$ mice coexpress Cre recombinase and GFP under the CD11c promoter. To measure GFP as a readout for Cre recombinase expression, the indicated splenic DC cell populations CD8α$^{+}$ DCs (CD8α$^{+}$Dec205$^{+}$CD11c$^{hi}$), CD4$^{+}$ DCs (CD8α$^{-}$Dec205$^{-}$CD11c$^{hi}$CD4$^{+}$), and pDCs (B220$^{+}$PDCA$^{+}$CD11c$^{int}$) as well as macrophages (F4/80$^{+}$CD11b$^{+}$) were analyzed by flow cytometry, and the mean fluorescence intensity (MFI) of GFP expression was determined. Shown is a summary of five mice from three independent experiments. (C) Decreased type I IFN sensitivity in CD8α$^{+}$ and CD4$^{+}$ DCs from *Itgax-Cre*$^{+}$*Ifnar1*$^{f/f}$ mice as determined by impaired CD86 up-regulation after stimulation with 10 ng/ml IFN-$\alpha_{v4}$ for 18 h. DCs were enriched using CD11c microbeads before stimulation. CD86 was measured by flow cytometry after gating on the indicated subsets. Shown is a summary of three independent experiments with mean fluorescence intensity of CD86 presented as a percentage relative to *Ifnar1*$^{f/f}$ (*, $P < 0.05$; **, $P < 0.01$). (B and C) Error bars represent SEM.

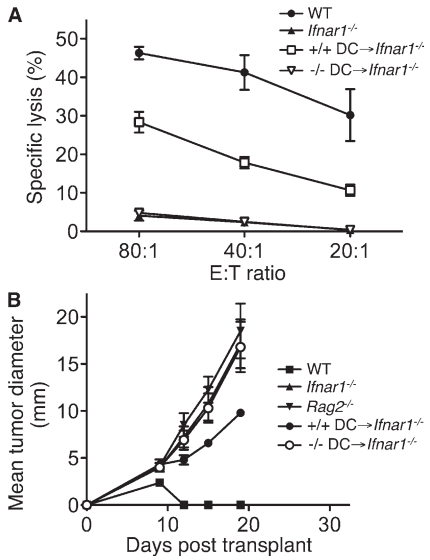


**Figure S9. Adoptive transfer of IFN-α/β–responsive CD11c$^{+}$ cells into *Ifnar1*$^{-/-}$ hosts partially reconstitutes tumor-specific CTL priming and affects tumor outgrowth.** Groups of WT and *Ifnar1*$^{-/-}$ control mice and *Ifnar1*$^{-/-}$ mice receiving WT or *Ifnar1*$^{-/-}$ CD11c$^{+}$ cells were challenged with $2 \times 10^{5}$ GAR4.GR1 tumor cells. (A) Splenocytes from these mice were harvested 20 d after GAR4.GR1 injection, co-cultured with IFN-γ–treated, irradiated GAR4.GR1 cells, and used 5 d later as effector cells in a cytotoxicity assay with $^{51}$Cr-labeled GAR4.GR1 targets. Specific killing activity (in percentage ± SEM) at the indicated effector/target (E:T) ratios is shown for two to three mice per group assayed in duplicate. The IFNAR1-deficient GAR4.GR1 tumor line was specifically used to ensure that potential priming of an anti-IFNAR1 immune response by transfer of WT cells into *Ifnar1*$^{-/-}$ mice could not contribute to tumor cell killing. Similar data were obtained in a second experiment. (B) Tumor growth was monitored over time in WT and *Ifnar1*$^{-/-}$ control mice and *Ifnar1*$^{-/-}$ mice receiving WT or *Ifnar1*$^{-/-}$ CD11c$^{+}$ cells and challenged with $2 \times 10^{5}$ GAR4.GR1 tumor cells. Shown is the mean tumor diameter ± SEM from four to five mice per group from one of three independent experiments. Using the Student's *t* test at day 19, $P = 0.03$ for WT CD11c$^{+}$ DCs → *Ifnar1*$^{-/-}$ versus *Ifnar1*$^{-/-}$ DCs → *Ifnar1*$^{-/-}$ recipients.

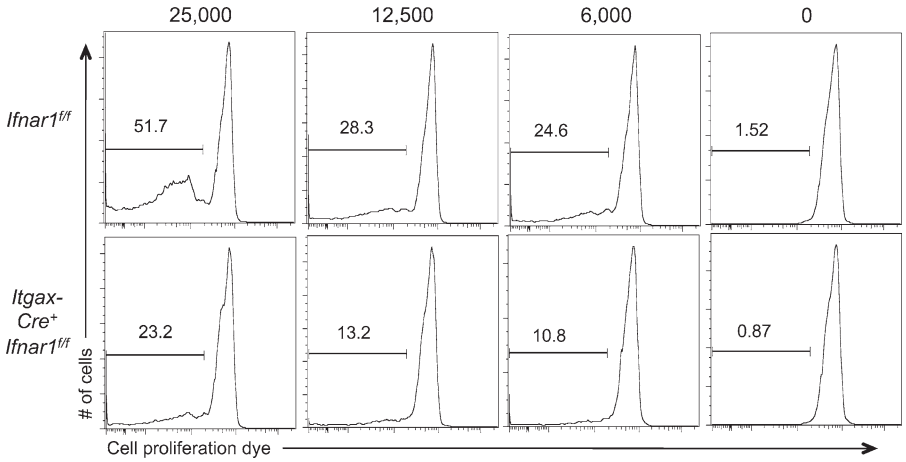


**Figure S10. *Itgax-Cre*$^{+}$*Ifnar1*$^{f/f}$ CD8$\alpha^{+}$ DCs exhibit reduced cross-presentation compared with *Ifnar1*$^{f/f}$ CD8$\alpha^{+}$ DCs when ovalbumin-transduced tumor cells are used as targets.** Purified CD8$\alpha^{+}$ DC subsets isolated from *Ifnar1*$^{f/f}$ or *Itgax-Cre*$^{+}$*Ifnar1*$^{f/f}$ mice were incubated with OT-I T cells labeled with cell proliferation dye and the indicated number of retrovirally transduced sarcoma cells expressing ovalbumin. Dilution of the cell proliferation dye was measured 3 d later. Data are representative of two independent experiments.